Acta Crystallographica Section F
Structural Biology and Crystallization Communications
ISSN 1744-3091

Crystallization and preliminary crystallographic analysis of mouse peroxiredoxin II with significant pseudosymmetry

Ari Ora,[a,b] Esko Oksanen,[a] Tommi Kajander,[a] Adrian Goldman[a] and Sarah J. Butcher[a,b]*

[a]Institute of Biotechnology, PO Box 65, 00014 University of Helsinki, Finland, and [b]Depart-Department of Biosciences, PO Box 65, 00014 University of Helsinki, Finland

Correspondence e-mail: sarah.butcher@helsinki.fi

Received 18 January 2010
Accepted 29 January 2010

Peroxiredoxin II was cloned from mouse B cells into pCold 1 expression vector and produced as a His-tagged recombinant protein in *Escherichia coli*. A ring form was isolated by gel filtration. A crystal obtained by the sitting-drop vapour-diffusion method diffracted to 1.77 Å resolution at 100 K. The crystal belonged to space group $P2_12_12$, with unit-cell parameters $a = 117.4$, $b = 133.9$, $c = 139.1$ Å. The asymmetric unit is expected to contain six dimers of peroxiredoxin II, with a corresponding solvent content of 39.3%. Peaks in the native Patterson function together with pseudo-systematic absences suggested that the crystals suffered from severe translational pseudosymmetry.

1. Introduction

Oxygen is essential for life but can be lethal to living organisms. Even under normal circumstances, the reduction of molecular O_2 during aerobic metabolism produces a range of reactive oxygen species (ROS) such as hydrogen superoxide radicals ($O_2^{-}\cdot$), hydroxyl radicals OH·) and hydrogen peroxide (H_2O_2). The cellular damage caused by oxidative stress has been associated with aging (Olahova *et al.*, 2008), many neurodegenerative diseases, such as Huntington's disease (Sorolla *et al.*, 2008), Parkinson's disease (Basso *et al.*, 2004), and breast cancer (Cha *et al.*, 2009). Cells have developed protective systems such as antioxidants, metal chelators and enzymatic reduction to protect themselves against these unwanted oxygen species (Finkel & Holbrook, 2000). The peroxiredoxins (Prxs) are a family of ubiquitous antioxidant enzymes that catalyze the reduction of hydrogen peroxide or alkyl peroxides to water or alcohols (Wood, Poole *et al.*, 2003; Wood, Schröder *et al.*, 2003; Schröder & Ponting, 1998). Cells also produce H_2O_2 for signalling and Prxs are thus involved in many intracellular signalling cascades (Budanov *et al.*, 2004) and the regulation of cell proliferation (Phalen *et al.*, 2006).

The six different Prx isoforms found in mammals are divided into three classes called 2-Cys Prxs (Prx I–IV), atypical 2-Cys Prxs (Prx V) and 1-Cys Prxs (Prx VI). They all contain a conserved active-site cysteine residue (peroxidatic cysteine) that is oxidized to sulfenic acid by H_2O_2. The 2-Cys Prxs contain a second conserved cysteine residue. The recycling of the sulfenic acid back to a thiol distinguishes the three enzyme classes: 2-Cys Prxs are reduced by thiols such as glutathione, while the 1-Cys enzymes may be reduced by ascorbic acid (Barranco-Medina *et al.*, 2009). The detailed catalytic cycle of the 2-Cys Prxs has been derived from crystal structures, including a model for the redox-regulated oligomeric state proposed to control enzyme activity. Inactivation of these enzymes by over-oxidation of the active thiol to sulfinic acid can be reversed by sulfiredoxin (Jonsson *et al.*, 2008).

The 2-Cys Prxs are obligate homodimers (Rhee *et al.*, 2005). However, several of them are also found as decamers. For example, the structure of human thioredoxin peroxidase (Schröder *et al.*, 2000) contained a decameric ring (Karplus & Hall, 2007). Other Prxs, such as HBP23, have been crystallized as dimers and decamers (Matsumura *et al.*, 2008). It has been shown in yeast that Prx I and PrxII may

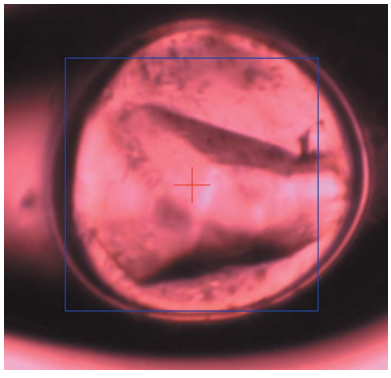

© 2010 International Union of Crystallography
All rights reserved

have a chaperone function when they form high-molecular-weight complexes in the cell (Jang *et al.*, 2004). This function has been confirmed in mammalian cells for Prx II. However, it is not yet known how Prx II binds the substrate or what conformational changes may occur during this process (Jang *et al.*, 2004; Moon *et al.*, 2005).

2. Methods and results

2.1. Cloning of Prx II

Total RNA was extracted from the mouse B-cell line I.29μ+ using Trizol (Invitrogen) according to the manufacturer's instructions. cDNA was obtained from 2 μg total RNA by reverse transcription PCR (RT-PCR) using M-MuLV reverse transcriptase and an oligo (dT)12–18 primer (Fermentas).

Gene-specific oligonucleotides were designed using a consensus sequence derived from mouse Prx II cDNAs in GenBank (Gene ID 21672). A PCR reaction was performed in 20 m*M* Tris–HCl pH 8.8, 10 m*M* KCl, 10 m*M* ammonium sulfate, 0.1% Triton X-100, 0.1 mg ml^{-1} bovine serine albumin, 1 μ*M* of each primer, 0.2 m*M* dNTPs, 2 m*M* $MgCl_2$, 5.2% dimethyl sulfoxide, 2 μl cDNA mix and 1 U *Pfu* DNA polymerase (Fermentas). The PCR program consisted of a pre-denaturation step at 367 K for 5 min followed by 30 cycles of amplification (denaturation at 367 K for 30 s, annealing at 328 K for 45 s and extension at 345 K for 2 min) and a final extension at 345 K for 10 min in a GeneCycler (Bio-Rad). A 0.6 kb RT-PCR product was obtained with the primer pair Prx2Nde1 (5′-GCCGCC**CATATG** GCATCCGGTAACGCGCAA-3′) and Prx2Xho1 (5′-GCCGCC**CTCGAG**TCAGTTGTGTTTGGAGAA-3′) (*Nde*I and *Xho*I sites in bold). The blunt PCR product was cloned into an *Eco*RV site in pBluescript SK− (Stratagene). DNA sequencing confirmed that the cDNA fragment encoded the full-length 198-amino-acid polypeptide, with 100% sequence similarity to GenBank entry AAH02034.1. The open reading frame (ORF) of Prx II was subcloned using the *Nde*I and *Xho*I restriction sites into a pCold1 prokaryotic expression vector with an N-terminal His tag (Takara) and transformed into *Escherichia coli* strain BL21 (DE3) (Novagen).

2.2. Overexpression and purification of mouse Prx II

To express mouse Prx II, a freshly transformed colony was used to inoculate 20 ml Terrific Broth supplemented with 100 μg ml^{-1} ampicillin at 310 K and grown overnight. This overnight starting culture was diluted 1:50 in the same medium and grown to an OD_{600} of ∼0.6; the culture was then cooled to 288 K on ice, followed by induction with 1 m*M* isopropyl β-D-1-thiogalactopyranoside. Induction continued for 2 d at 288 K. The cells were harvested by centrifugation at 3200*g* for 10 min at 277 K and the cell pellets were resuspended in 50 m*M* NaCl, 1 m*M* dithiothreitol (DTT), 25 m*M* Bicine pH 8.2 (buffer *A*). Cells were disrupted with a French press (Thermo) at 281 K. Cell debris was removed by centrifugation at 16 887*g* for 10 min at 277 K. The recombinant protein was concentrated by mixing 20 ml supernatant with 5 ml of a slurry of IMAC beads (GE Healthcare) preloaded with nickel ions and stirring for 0.5 h at 277 K. The IMAC beads were pelleted by centrifugation and washed in a head-to-head rotator with 150 ml buffer *A*. The Prx II was eluted three times (5 ml each time) with buffer *A* supplemented with 0.25 *M* ethylenediaminetetraacetic acid and 0.27 *M* imidazole. The eluates were concentrated and the buffer was exchanged to buffer *A* by ultrafiltration (Amicon Ultra-4, 10 kDa cutoff, Millipore) to an end volume of 1.5 ml. The sample was then applied onto a HiTrap Q HP anion-exchange column (GE Healthcare), the column was washed with buffer *A* until the baseline was stable and the Prx II was eluted using a linear 50 m*M*–1 *M* NaCl gradient in 1 m*M* DTT, 25 m*M* Bicine pH 8.2. The eluted protein was concentrated and applied onto a Sephadex 75 (GE Healthcare) gel-filtration column in buffer *A*. The presumed ring form of Prx II was collected and concentrated by ultrafiltration (Amicon Ultra-4, 10 kDa cutoff, Millipore).

2.3. Crystallization and X-ray data collection.

Purified Prx II at a concentration of 20 mg ml^{-1} in 20 m*M* Bicine pH 8.2, 50 m*M* NaCl, 1 m*M* DTT was used to screen for crystallization conditions in Innovadyne SD-2 crystallization plates using the sitting-drop vapour-diffusion method with 80 μl reservoir solution in the wells and drops containing 0.1 μl protein solution and 0.1 μl reservoir solution at 295 K. A combined sparse-matrix and incomplete factorial screen was used covering pH 3.5–8.5, low ionic strength, high ionic strength, mixed polymer/salt conditions and

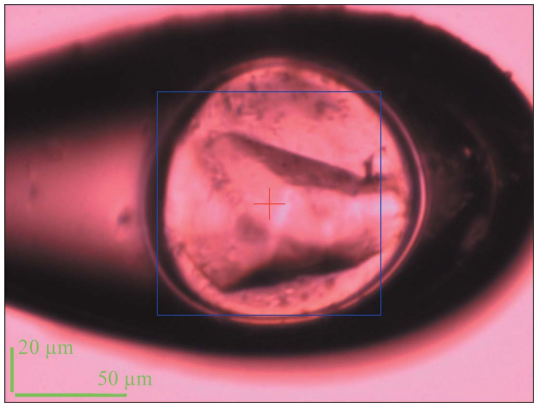

Figure 1
A *Mus musculus* Prx II crystal flash-cooled in a loop with Paratone-N oil.

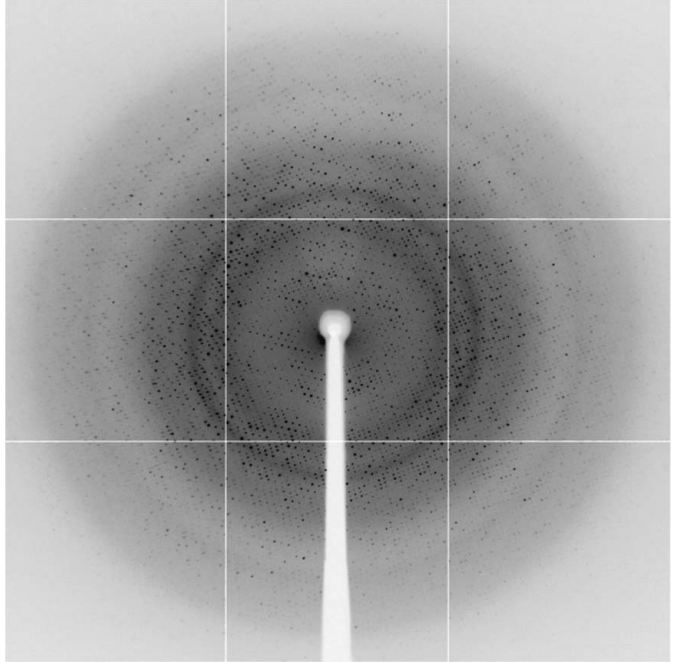

Figure 2
X-ray diffraction image from a *M. musculus* Prx II crystal. The edge of the detector is set at 1.77 Å resolution.

Table 1
Data-collection statistics.

Values in parentheses are for the highest resolution shell.

Wavelength (Å)	1.0332
Space group	$P2_12_12$
Unit-cell parameters (Å)	a = 117.6, b = 133.9, c = 139.1
Resolution (Å)	1.77 (1.89–1.77)
No. of measured reflections	1416870 (247687)
No. of unique reflections	207550 (35677)
Redundancy	6.7 (6.9)
Completeness (%)	95.3 (93.5)
$\langle I/\sigma(I)\rangle$	7.7 (2.6)
$R_{\rm merge}$† (%)	20.0 (75.3)

† $R_{\rm merge} = \sum_{hkl}\sum_i |I_i(hkl) - \langle I(hkl)\rangle| / \sum_{hkl}\sum_i I_i(hkl)$, where $I_i(hkl)$ is the ith intensity measurement of reflection hkl, including symmetry-related reflections, and $\langle I(hkl)\rangle$ is its mean.

Table 2
Peaks in the native Patterson map.

x	0.50	0	0.50
y	0.50	0.42	0.09
z	0	0.50	0.50
% of origin peak	15.7	53.0	8.1

halides for potential phasing (http://www.biocenter.helsinki.fi/bi/X-ray/automation/services.htm). Larger drops were then set up from positive hits using the same protein concentration and buffer. The protein crystallized at 295 K in 0.1 *M* 4-(2-hydroxyethyl)-1-piperazineethanesulfonic acid pH 7.5, 1.4 *M* sodium citrate from sitting drops consisting of 2 µl mother liquor and 2 µl protein solution. Small crystals of ∼100 µm in length grew slowly within a month. A single crystal was flash-cooled in liquid nitrogen with Paratone-N as a cryoprotectant (Fig. 1). The crystal diffracted to high resolution (Fig. 2) and a data set was collected to 1.77 Å resolution on beamline ID23-1 at the European Synchrotron Radiation Facility (ESRF). Data were processed with the *XDS* package (Kabsch, 1993; Table 1). The data were indexed in a primitive orthorhombic lattice with unit-cell parameters a = 117.6, b = 133.9, c = 139.1 Å. $P2_12_12$ is the most likely space group based on systematic absences. In addition, the native Patterson function has three major peaks (Table 2), suggesting the presence of translational noncrystallographic symmetry (see §3).

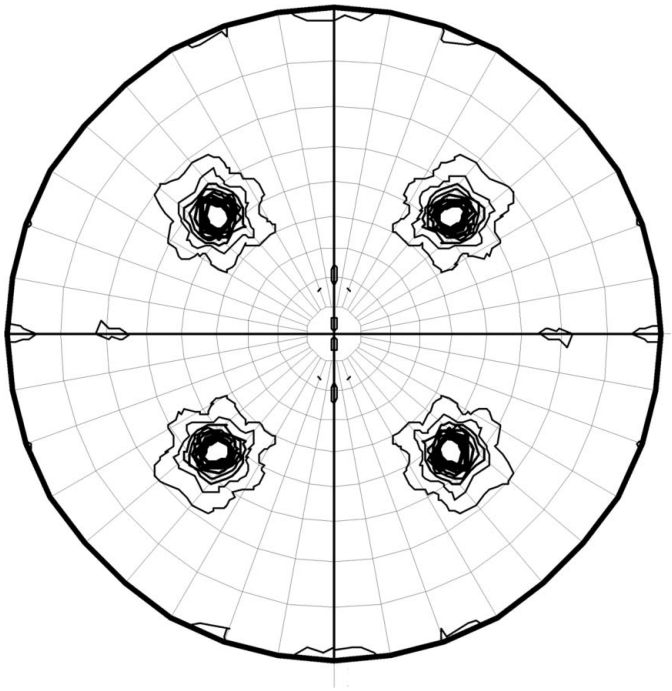

Figure 3
Self-rotation function for $\kappa = 120^\circ$ for Prx II data (20–30 Å resolution range). The plot was generated with *MOLREP* (Vagin & Teplyakov, 1997).

Table 3
Intensity ratios for reflections with $h + k$, $k + l$ or $h + l$ odd or even.

Reflection condition	$h + k$	$k + l$	$h + l$
No. of odd reflections	411207	409896	410277
No. of even reflections	408811	410122	409741
$\langle I_{\rm odd}\rangle/\langle I_{\rm even}\rangle$	0.39	0.848	0.827

3. Discussion

Protein structures with highly similar sequences to that of mouse PrxII are available (Hirotsu *et al.*, 1999; Matsumura *et al.*, 2008; Schröder *et al.*, 2000) and therefore molecular replacement should be straightforward. On the other hand, the structure solution and refinement of heavily pseudo-symmetric structures (Zwart *et al.*, 2008) can be very challenging even if a practically identical model is available (Oksanen *et al.*, 2006). Ring structures such as those observed for other published Prx ring structures (Schröder *et al.*, 2000) should produce sixfold or fivefold peaks in the self-rotation function at $\kappa = 60^\circ$ or 72°, as has been reported. This is inconsistent with the threefold NCS observed here. In the self-rotation function the most significant peaks after the origin peaks are at $\kappa = 120^\circ$ (Fig. 3). The next highest peaks are twofold rotations (not shown). Analysis of the Matthews coefficient suggests that there are six dimers of Prx in the asymmetric unit (solvent content 39.3%, $V_{\rm M}$ = 2.03 Å^3 Da^{-1}).

Translational pseudosymmetry is known to significantly complicate structure solution and refinement even when only one pseudo-translation vector is present. Here, analysis of the pseudosymmetry and its relation to crystallographic symmetry is far more complicated.

The native Patterson function has three significant non-origin peaks (Table 2). The peak at $y \simeq 0.5$, $z \simeq 0.5$ was particularly strong. Parity analysis indicated that reflections of the form $h + k = 2n + 1$ were systematically weak compared with the other potential absences (Table 3). The ratio $\langle I_{(h+k\,=\,2n+1)}\rangle/\langle I_{(h+k\,=\,2n)}\rangle$ of 0.39 suggests pseudo-*C*-face centring, but the highest peak at $x = 0$, $y = 0.42$, $z = 0.5$ would, however, correspond to *A*-centring. The explanation is that $z = 0.42$ is sufficiently far from 0.5 so that the intensity ratio is not significantly affected even though the Patterson peak is high. On the other hand, the next highest Patterson peak at $x = 0.5$, $y = 0.5$, $z = 0$ corresponds to pseudo-*C*-centering. The intensity ratios for reflections with $h + l$ and $k + l$ (Table 3) also differ from the expected value of 1.0, although not as drastically as with $h + k$.

Despite the availability of high-sequence similarity models, molecular-replacement trials have so far failed to yield a solution that is consistent with the observed rotational and translation NCS. Trials in lower symmetry space groups including *P*1 have been similarly unsuccessful and attempts to obtain experimental phase information are in progress.

We thank Dr Roberto de Sitia for the generous gift of the mouse B-cell line I.29µ+, Dr Ineke Braakman for sharing information on the B-cell screen and Seija Mäki for help with crystallization. This work was supported by the Sigrid Juselius Foundation (SJB, AG), Biocenter Finland (SJB), the Academy of Finland Centre of Excellence in Virus Research (2006–2011; 1129684, SJB), a postdoctoral

fellowship from the Academy of Finland (TK) and the National Graduate School for Informational and Structural Biology (EO). Beamtime was provided by the European Synchrotron Radiation Facility.

References

Barranco-Medina, S., Lazaro, J. J. & Dietz, K. J. (2009). *FEBS Lett.* **583**, 1809–1816.
Basso, M., Giraudo, S., Corpillo, D., Bergamasco, B., Lopiano, L. & Fasano, M. (2004). *Proteomics*, **4**, 3943–3952.
Budanov, A. V., Sablina, A. A., Feinstein, E., Koonin, E. V. & Chumakov, P. M. (2004). *Science*, **304**, 596–600.
Cha, M. K., Suh, K. H. & Kim, I. H. (2009). *J. Exp. Clin. Cancer Res.* **28**, 93.
Finkel, T. & Holbrook, N. J. (2000). *Nature (London)*, **408**, 239–247.
Hirotsu, S., Abe, Y., Okada, K., Nagahara, N., Hori, H., Nishino, T. & Hakoshima, T. (1999). *Proc. Natl Acad. Sci. USA*, **96**, 12333–12338.
Jang, H. H. *et al.* (2004). *Cell*, **117**, 625–635.
Jonsson, T. J., Murray, M. S., Johnson, L. C. & Lowther, W. T. (2008). *J. Biol. Chem.* **283**, 23846–23851.
Kabsch, W. (1993). *J. Appl. Cryst.* **26**, 795–800.
Karplus, P. A. & Hall, A. (2007). *Subcell. Biochem.* **44**, 41–60.
Matsumura, T., Okamoto, K., Iwahara, S., Hori, H., Takahashi, Y., Nishino, T. & Abe, Y. (2008). *J. Biol. Chem.* **283**, 284–293.
Moon, J. C., Hah, Y. S., Kim, W. Y., Jung, B. G., Jang, H. H., Lee, J. R., Kim, S. Y., Lee, Y. M., Jeon, M. G., Kim, C. W., Cho, M. J. & Lee, S. Y. (2005). *J. Biol. Chem.* **280**, 28775–28784.
Oksanen, E., Jaakola, V.-P., Tolonen, T., Valkonen, K., Åkerström, B., Kalkkinen, N., Virtanen, V. & Goldman, A. (2006). *Acta Cryst.* D**62**, 1369–1374.
Olahova, M., Taylor, S. R., Khazaipoul, S., Wang, J., Morgan, B. A., Matsumoto, K., Blackwell, T. K. & Veal, E. A. (2008). *Proc. Natl Acad. Sci. USA*, **105**, 19839–19844.
Phalen, T. J., Weirather, K., Deming, P. B., Anathy, V., Howe, A. K., van der Vliet, A., Jonsson, T. J., Poole, L. B. & Heintz, N. H. (2006). *J. Cell Biol.* **175**, 779–789.
Rhee, S. G., Chae, H. Z. & Kim, K. (2005). *Free Radic. Biol. Med.* **38**, 1543–1552.
Schröder, E., Littlechild, J. A., Lebedev, A. A., Errington, N., Vagin, A. A. & Isupov, M. N. (2000). *Structure*, **8**, 605–615.
Schröder, E. & Ponting, C. P. (1998). *Protein Sci.* **7**, 2465–2468.
Sorolla, M. A., Reverter-Branchat, G., Tamarit, J., Ferrer, I., Ros, J. & Cabiscol, E. (2008). *Free Radic. Biol. Med.* **45**, 667–678.
Vagin, A. & Teplyakov, A. (1997). *J. Appl. Cryst.* **30**, 1022–1025.
Wood, Z. A., Poole, L. B. & Karplus, P. A. (2003). *Science*, **300**, 650–653.
Wood, Z. A., Schröder, E., Harris, J. R. & Poole, L. B. (2003). *Trends Biochem. Sci.* **28**, 32–40.
Zwart, P. H., Grosse-Kunstleve, R. W., Lebedev, A. A., Murshudov, G. N. & Adams, P. D. (2008). *Acta Cryst.* D**64**, 99–107.